Acta Biochim Biophys Sin 2025, 57(x): 1–15
https://cstr.cn/32197.14.abbs.2025158
https://doi.org/10.3724/abbs.2025158
Original Article

Original Article

The E2F1–KIF14 axis drives focal adhesion formation and promotes colorectal cancer metastasis

Yajie Wang, Xinyue Wu, Xiaofeng Li, Xiaoying Lian, Jiao An, Wenhua Cai, Jing Jia, and Changjun Zhu*

Tianjin Key Laboratory of Animal and Plant Resistance, College of Life Sciences, Tianjin Normal University, Tianjin 300387, China
*Correspondence address. Tel: 86-22-23760711 E-mail: skyzcj@tjnu.edu.cn.

Received 16 July 2025 Accepted 19 August 2025 Published 10 September 2025

Abstract

Kinesin family member 14 (KIF14) has been implicated in the progression of multiple cancer types, yet its role in colorectal cancer (CRC) metastasis remains undefined. Here, we assesse KIF14 expression in CRC specimens and explore its clinical and functional significance. KIF14 upregulation is frequently observed in CRC tissues and is correlated with advanced tumor stage and reduced overall survival. Functional assays reveal that KIF14 depletion in CRC cells inhibits migration, invasion, and *in vivo* metastatic colonization, whereas KIF14 overexpression induces the opposite effects. Transcriptomic and pathway enrichment analyses reveal that KIF14 functions as a critical regulator of focal adhesion and cell-matrix adhesion signaling. This finding is further supported by experimental evidence showing that KIF14 overexpression promotes focal adhesion assembly, whereas *KIF14* knockdown disruptes this process. Mechanistically, we demonstrate that KIF14 binds directly to the focal adhesion protein vinculin and mediates its delivery to the leading edge of migrating cells. Moreover, bioinformatics prediction and chromatin immunoprecipitation confirm that E2F1 directly binds the *KIF14* promoter to drive its transcription. Rescue experiments reveal that ectopic KIF14 expression restores the prometastatic phenotypes suppressed by *E2F1* silencing, indicating that the effects of E2F1 are mediated by the E2F1–KIF14 axis. Collectively, our findings reveal a novel E2F1–KIF14–vinculin signaling axis that drives CRC metastasis by modulating focal adhesion dynamics, highlighting KIF14 as a potential therapeutic target.

Key words colorectal cancer, metastasis, KIF14, E2F1, focal adhesion

Introduction

Colorectal cancer (CRC), a malignancy originating from the mucosal epithelium, accounted for 1.9 million new cancer cases and 903,000 related deaths in 2022 (IARC), ranking the third in incidence and second in mortality worldwide [1]. Two alarming trends have recently been observed for CRC: a dramatic surge in early-onset cases, with the incidence among individuals under 50 years rising by 50% over three decades, and an aggressive metastatic propensity [2,3]. Notably, 20% of patients present with distant metastases at initial diagnosis, whereas over 50% develop metastases during disease progression [3]. The dismal five-year survival rate of patients with metastatic CRC (less than 15%) underscores the critical need to decipher the molecular mechanisms driving tumor dissemination.

Kinesin family member 14 (KIF14), a microtubule-directed motor protein belonging to the kinesin-3 family, is increasingly recognized for its multifaceted role in cancer biology. Its distinctive structural features, including an N-terminal motor domain for ATP-dependent movement, coiled-coil domains facilitating dimerization, and a neck-linker region for directional transport, suggest that KIF14 may act as a critical regulator of cytoskeletal dynamics [4–7]. While it was initially found to play a role in cytokinesis, KIF14 is now recognized as an oncogenic driver in multiple malignancies, and its aberrant expression correlates with aggressive tumor progression, enhanced metastatic potential, and therapeutic resistance [8–10].

Previous studies have revealed diverse mechanisms through which KIF14 promotes cancer progression. In breast cancer, KIF14 promotes cell migration and invasion by modulating the Rap1–Radil signaling pathway [11]. In gastric cancer, it influences AKT-mediated epithelial–mesenchymal transition (EMT), and in eso-

phageal squamous cell carcinoma, it maintains metastatic capability by interacting with mitochondrial proteins [12,13]. Previous studies have shown that KIF14 promotes CRC cell proliferation by activating the Akt signaling pathway and acts as a direct target of miR-200c [14,15]. However, its role in CRC metastasis remains unclear.

Focal adhesions play crucial roles in tumor migration and invasion by regulating cell–extracellular matrix (ECM) adhesion and transmitting mechanical signals that promote tumor cell motility and infiltration [16]. Various proteins within focal adhesions, including integrins, focal adhesion kinase (FAK), and Src, activate multiple downstream signaling pathways that orchestrate cell migration, matrix remodeling, and angiogenesis, thereby increasing tumor cell invasiveness [17–19]. Moreover, focal adhesions participate in remodeling the tumor microenvironment by promoting ECM degradation and reorganization, creating favorable conditions for tumor cell dissemination. The dynamic assembly and disassembly of focal adhesions further enable tumor cells to effectively traverse tissue barriers during metastasis, facilitating their directional movement and invasion. Intriguingly, previous studies have demonstrated that KIF14 colocalizes with supervillin (SVIL), a membrane-microfilament binding protein that regulates pseudopodia formation and cellular motility through its interactions with myosin II and cortactin [20]. This spatial association suggests a potential mechanistic link whereby KIF14 modulates focal adhesion dynamics to influence cell migration.

In this study, we investigated the critical role and regulatory mechanisms of KIF14 in CRC. Clinical data revealed that KIF14 is markedly upregulated in CRC tissues and is associated with aggressive disease progression, suggesting its potential value as a prognostic marker. Mechanistically, we revealed that KIF14 enhances cancer cell migration, invasion, and EMT by orchestrating focal adhesion dynamics, with our data demonstrating a direct interaction with vinculin, a key focal adhesion protein. At the transcriptional level, we established E2F1 as a direct activator of KIF14 expression, thus connecting the well-documented prometastatic functions of E2F1 to KIF14-mediated motility regulation. For the first time, these findings establish the E2F1–KIF14 axis as a signaling cascade involved in CRC metastasis, providing new ideas for the development of therapeutic strategies aimed at limiting metastatic dissemination.

Materials and Methods

Cell culture

HCT116, SW620, Lovo, Caco-2, SW480, FHC, and HEK-293T cells (ATCC, Manassas, USA) were maintained at 37 °C with 5% CO_2 as follows: SW480/HEK-293T in DMEM (Hyclone, Logan, USA) + 10% FBS (JYK, Guangzhou, China); Caco-2 in MEM (Meilun Bio, Dalian, China) + 10% FBS; SW620 in L15 (Servicebio, Wuhan, China) + 10% FBS; HCT116 in RPMI 1640 (Servicebio) + 10% FBS; and Lovo/FHC in DMEM/F-12 (Servicebio) + 10% FBS.

Plasmids and siRNAs

The full-length cDNAs of human *E2F1* and *KIF14* were generated via PCR and subcloned into the pFLAG mammalian expression vector. Full-length vinculin cDNA was seamlessly cloned into the pcDNA3.1-HA vector. Gene-specific siRNAs were designed and synthesized by GenePharma (Shanghai, China) with the following sequences: siNC: 5′-UUCUCCGAACGUGUCACGUTT-3′; siE2F1: 5′-UAACUGCACUUUCGGCCCUTT-3′; and siKIF14: 5′-AACCUGAUCC UUUCAUUUGCC-3′.

Clinical specimens

A tissue microarray (TMA), which included 62 pairs of colon adenocarcinoma (COAD) tissue samples alongside corresponding normal tissue samples, was purchased from Wuhan Servicebio Technology. Immunohistochemistry (IHC) was performed using an anti-KIF14 antibody (a10275; ABclonal, Wuhan, China). The IHC process was complemented by automated quantitative analysis. The stained slides were independently examined via ImageJ software (Java 8).

Bioinformatics analysis

The differential expression and correlation of KIF14 in CRC were assessed via COLONOMICS (https://www.colonomics.org/), including 100 paired tumor and adjacent normal tissues from stage II colon cancer patients and 50 healthy colon mucosa samples, resulting in 250 samples analyzed throughout the study [21]. Overall survival associations were evaluated in 841 patients via Kaplan-Meier Plotter (median split; https://www.kmplot.com/analysis/), which integrates gene expression and survival data from public datasets including TCGA, GEO, and EGA [22].

Cell transfection

HCT116 and SW480 cells were seeded in 6-well plates at 2×10^5 cells/well 24 h before transfection. Transfections were performed via Lipo8000™ reagent (Beyotime, Shanghai, China) according to the manufacturer's protocol. For siRNA transfection, 50 nM siRNA was used. For plasmid transfection, 2 μg of expression vector or empty vector was used. For co-transfection, 50 nM siRNA and 2 μg of plasmid were mixed with Lipo8000™ (Beyotime) in Opti-MEM (Meilun Bio), incubated for 10 min, and added to the cells. The medium was replaced after 6 h, and the cells were harvested 48 h post-transfection.

Western blot analysis

The cells were lysed in RIPA buffer (50 mM Tris-HCl pH 7.4, 150 mM NaCl, 1% Triton X-100, 0.1% SDS, 10% glycerol) supplemented with protease inhibitors. Protein (40 μg) was resolved via 7.5–10% SDS-PAGE, transferred to PVDF membranes, blocked in 10% non-fat milk/TBS (50 mM Tris-Cl, pH 7.5; 200 mM NaCl) for 1 h, and then incubated with primary antibodies at room temperature for 2 h. Primary antibodies against α-tubulin and FLAG (M2; Sigma-Aldrich, St. Louis, USA), vinculin (ab129002; Abcam, Cambridge, UK), vimentin, N-cadherin, E-cadherin and KIF14 (a19607, a19083, a20798, a10275; ABclonal), E2F1 (ET1701-73; Huaan, Hangzhou, China), and β-actin (Servicebio) were used. HRP-conjugated goat anti-rabbit/mouse IgG (31430/31460, Invitrogen, Carlsbad, USA) and enhanced chemiluminescence (ECL) reagents (Beyotime) were used for band detection. Band intensities were quantified via ImageJ (Java 8).

Immunofluorescence (IF) assay

The cells were grown for 24 h, washed in PBS, fixed in 4% paraformaldehyde (Beyotime) for 20 min, permeabilized with 0.1% Triton X-100 (Solarbio, Beijing, China) for 5 min, blocked in 5% serum albumin, and then incubated with primary antibody overnight (4 °C). After a 1-h incubation with a fluorophore-conjugated

secondary antibody, the nuclei were stained with DAPI (Solarbio) for 3 min. Images were acquired with a Nikon A1 confocal microscope.

Wound healing assay

A total of 1×10^5 cells/well were plated in 6-well plates and serum-starved overnight. A scratch was made with a 200-μL tip; the debris was removed with PBS, and the cells were maintained in 0.5% BSA/serum-free medium. Migration was imaged under a light microscope (Nikon, Tokyo, Japan) at 0 and 48 h.

Matrigel invasion assay

Transwell inserts were coated with Matrigel diluted in serum-free DMEM (3 h, 37 °C). A total of 5×10^5 cells in 200 μL of serum–free medium were added to the upper chamber; the lower chamber contained medium supplemented with 10% FBS. After 48 h (37 °C, 5% CO_2), non-invading cells were removed; invading cells were fixed (4% paraformaldehyde), stained with crystal violet, and counted in five random fields.

Lentiviral vector preparation and transduction

pLKO.1-puro vectors carrying KIF14-targeting or control shRNAs were co-transfected with psPAX2 and pMD2. G into HEK293T cells via polyethyleneimine (PEI). Viral supernatant was used to transduce SW480 cells, which were selected with puromycin for 48 h to generate stable knockdown and control lines.

Stable cell line generation

Stable KIF14-overexpressing cell lines were generated following a previously described protocol [23]. Briefly, SW480 cells were transfected with pFLAG-KIF14 via Lipo8000™ and selected in DMEM + 10% FBS supplemented with 100 μg/mL G418 (Beyotime) for 15–21 days. Individual G418-resistant clones were expanded, and KIF14 overexpression was confirmed by western blot analysis. For knockdown, cells were infected with lentivirus carrying KIF14-targeting shRNA in the presence of 8 μg/mL polybrene and then selected with 2 μg/mL puromycin for 7 days; the knockdown efficiency was likewise verified by western blot analysis.

RNA sequencing

Total RNA from stable shKIF14 and control (shNC) SW480 lines was extracted with TRIzol (Servicebio). Library preparation, sequencing, and bioinformatics processing (differentially expressed genes [DEGs] identified as genes with FDR < 0.05, $|FC| \geq 2$; GO and KEGG enrichment analyses conducted via Novelbio's online platform) were performed by Shanghai Novelbio Ltd. GSEA was conducted via GSEA v4.3.2.

Co-immunoprecipitation (Co-IP)

293T cells were transiently transfected with the indicated plasmids. After 48 h, the cells were lysed in IP lysis buffer (50 mM Tris-HCl pH 7.4, 150 mM NaCl, 1% NP-40, and 1 mM EDTA supplemented with protease inhibitors). The lysates were clarified by centrifugation at 14,000 *g* for 15 min at 4°C.

For immunoprecipitation, the cleared lysates were incubated overnight at 4°C with either M2 FLAG beads (M8823, Sigma) for Flag-KIF14 pull-down or with anti-HA antibody (AE105, ABclonal) followed by protein A/G agarose beads for HA-vinculin pull-down. The beads were subsequently washed five times with IP lysis buffer. Bound proteins were eluted by boiling in 1× SDS sample buffer and detected by western blot analysis with specific antibodies.

qRT–PCR

Total RNA was extracted from siRNA- or plasmid-transfected cells via TRIzol. cDNA was synthesized from 1 μg of RNA via the GoScript™ Reverse Transcription System (Promega, Madison, USA). qRT–PCR was performed using SYBR Green Master Mix (Vazyme, Nanjing, China). The primer sequences are listed in Supplementary Table S1.

In silico promoter analysis

The KIF14 TSS (chr1q32.1) was defined by aligning the 5′ upstream transcript (NM_001305792.1) to the human genome via NCBI BLAST. TF-binding motifs in the ∼2 kb promoter region were predicted via JASPAR 2024 (score > 80%, similarity > 0.85) and Human TFDB v4.0 ($P < 1\times10^{-5}$, conservation > 5) [24,25].

ChIP assay

The cells in culture were cross-linked (1% formaldehyde, 15 min) and quenched with glycine, and the nuclei were isolated in ChIP buffer (50 mM HEPES-KOH, 140 mM NaCl, 1 mM EDTA, 1% Triton X-100, 0.1% sodium deoxycholate, 0.1% SDS, supplemented with protease inhibitors). Chromatin was sonicated, immunoprecipitated with IgG or anti-E2F1, and captured on protein A/G beads. After washing and de-crosslinking (10% Chelex 100, Bio-Rad Laboratories, Hercules, USA), the DNA was purified and analyzed via PCR and agarose gel electrophoresis.

Site-directed mutagenesis

The full-length *KIF14* promoter in pGL3-KIF14 was obtained from GENEWIZ. E2F1-binding site deletions (pGL3-KIF14-prom-mut) were generated via QuickChange (Stratagene, Santa Clara, USA). The plasmid pFLAG-E132, which disrupts the DNA-binding domain of E2F1, was generated by introducing L132E and N133S mutations into the wild-type *E2F1* sequence, as previously reported [26]. All the constructs were confirmed by sequencing. The primer sequences are provided in Supplementary Table S2.

Luciferase reporter gene assay

The three mutant promoter sequences of *KIF14* with mutations in the E2F1 binding site were subsequently cloned and inserted into the pGL3-Basic vector. The cells were seeded into 24-well plates at a density of 5×10^3 cells/well. The recombinant pGL3-Basic vector and E2F1 overexpression (pFLAG-E2F1) or negative control (NC) plasmids were cotransfected into the cells. After 48 h, the cells were lysed, and according to the manufacturer's instructions, a dual luciferase reporter analysis system (Promega) was used to detect the optical density.

Animal experiments

Female BALB/C nude mice, aged 3 to 4 weeks, were obtained from Beijing SPFbiotech Co., Ltd (Beijing, China). Mice were housed in a specific pathogen-free (SPF) facility, under a 12 h light/12 h dark cycle, at 22–25 °C, with 50–60% relative humidity, and had free access to sterilized food and water. All procedures were approved by the Tianjin Normal University Animal Ethics Committee and performed under SPF conditions (No. 2025022804). Nude mice ($n = 5$ per group) received tail-vein injections of 1.5×10^6 KIF14-overexpressing or control cells. After euthanasia, the lungs were

harvested, and metastatic nodules were counted.

Hematoxylin and eosin (H&E) staining

Tissue samples were fixed in 4% paraformaldehyde (Beyotime), embedded in paraffin, and sectioned at 4 μm. Sections were deparaffinized, rehydrated, and stained with hematoxylin and eosin (Solarbio) following standard protocols. After dehydration and mounting, images were captured under a light microscope (Nikon).

Statistical analysis

Data are presented as the mean ± SD. Two-group comparisons were performed via Student's *t*-test, whereas multi-group analyses were performed via one-way ANOVA with Tukey's post hoc test (GraphPad Prism). $P < 0.05$ was considered to indicate statistical significance.

Results

Aberrant expression and clinical significance of KIF14 in colorectal cancer

To comprehensively characterize the expression profile and clinical relevance of KIF14 in CRC, we conducted an integrated analysis of public database mining and experimental data. Analysis of the Colonomics database (which includes information on 100 tumor/adjacent tissue pairs and 50 healthy tissue samples) revealed significantly elevated KIF14 mRNA levels in tumor tissues compared with both adjacent nontumor tissues and healthy mucosa ($P < 0.001$; Figure 1A). This upregulation was clinically significant,

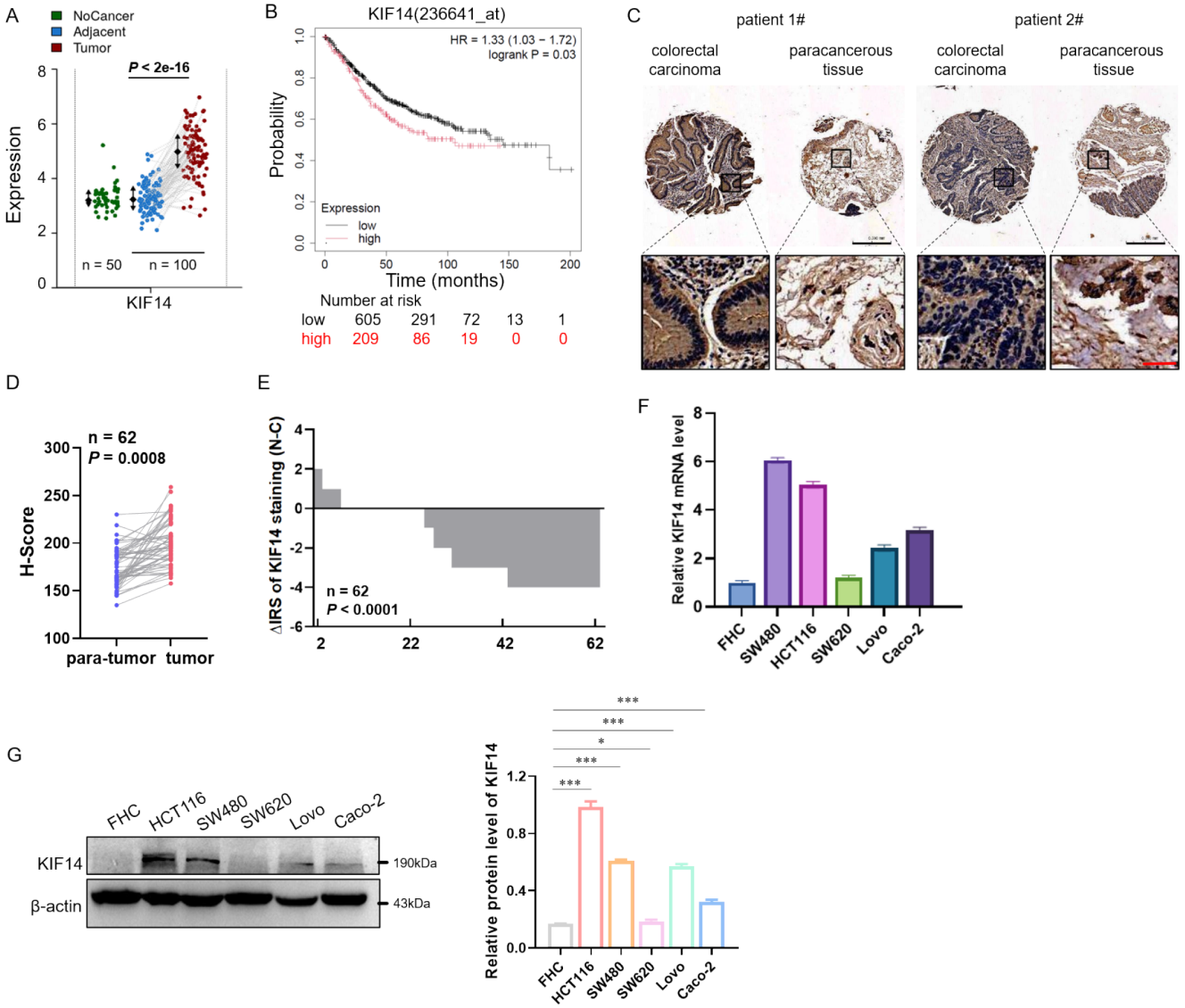

Figure 1. Increased KIF14 expression in colorectal cancer is correlated with poor prognosis (A) KIF14 mRNA expression levels in CRC tissues, adjacent nontumor tissues, and healthy control samples obtained from the Colonomics database. (B) Kaplan–Meier analysis of overall survival in CRC patients ($n = 814$) grouped by KIF14 expression levels. (C) Representative immunohistochemistry images depicting KIF14 expression in paired samples of CRC and adjacent nontumor tissues. Scale bar: 0.2 mm (black) and 50 μm (red). (D,E) Quantification of KIF14 protein expression according to the H-Score (D) and IRS (E) systems in paired tissues ($n = 62$ pairs). (F) mRNA levels of *KIF14* in CRC cell lines and normal colonic epithelial cells (the FHC cell line) were assessed via qRT–PCR. (G) The protein expression levels of KIF14 in CRC cell lines and FHC cells were assessed via western blot analysis. * $P < 0.05$, ** $P < 0.01$, *** $P < 0.001$.

as Kaplan–Meier survival analysis of 814 CRC patients demonstrated that patients with high KIF14 expression presented significantly shorter overall survival than did those with low KIF14 expression (log-rank test, $P < 0.001$; Figure 1B).

To validate these findings at the protein level, we performed immunohistochemical analysis of 62 paired colorectal adenocarcinoma samples (tumor) and adjacent nontumor tissues (paratumor). KIF14 protein expression, quantified via the H-Score and IRS scoring systems, was significantly greater in tumor tissues than in matched control tissues ($P < 0.001$; Figure 1C–E). Clinicopathological correlation analysis revealed a strong positive association between KIF14 expression and advanced tumor stage ($P < 0.05$; Table 1), although no significant correlations were detected between KIF14 expression and age, sex, or lymph node metastasis ($P > 0.05$).

To validate these findings at the cellular level, western blot and qRT–PCR analyses were performed. The experiments consistently demonstrated elevated KIF14 expression across multiple CRC cell lines (HCT116, SW480, SW620, LoVo, and Caco-2) compared with that in normal human colonic epithelial cells (the FHC cell line) ($P < 0.01$; Figure 1F–G). The HCT116 and SW480 cells presented the highest KIF14 levels, making them optimal models for subsequent functional investigations. These findings suggest that KIF14 upregulation is a key driver of CRC progression.

KIF14 promotes colorectal cancer cell motility and metastasis *in vitro* and *in vivo*

We generated stable HCT116 and SW480 cell lines overexpressing Flag-tagged KIF14 via plasmid transfection and confirmed robust induction via western blot analysis (Figure 2A). Moreover, *KIF14* knockdown was achieved via the use of a siRNA targeting the 3′ UTR, and western blot analysis confirmed efficient protein depletion (Figure 2B). Compared with control cells, KIF14-overexpressing cells presented increased migratory capacity with faster wound closure (Figure 2C–D), whereas *KIF14*-knockdown cells (both HCT116 and SW480) exhibited impaired cell motility (Figure 2E–F). Consistently, Matrigel-coated Transwell assays revealed a marked increase in the number of invading HCT116 and SW480 cells upon KIF14 overexpression after 48 h (Figure 2G–H). Conversely, *KIF14* knockdown markedly reduced the number of invaded cells in both cell lines (Figure 2I–J). These findings demonstrate that KIF14 plays a critical role in promoting colorectal cancer cell motility and invasiveness, supporting its function as a key driver of metastasis.

Next, we aimed to evaluate the *in vivo* metastatic potential of KIF14. SW480 cell lines stably expressing Flag-KIF14 or empty vector were established (Supplementary Figure S1) and injected via the tail vein into immunodeficient mice. Compared with control mice, mice injected with Flag-KIF14 cells developed significantly more pulmonary metastatic nodules ($P < 0.01$; Figure 2K–L). Hematoxylin and eosin (H&E) staining of lung sections confirmed a greater density and larger size of metastases in the KIF14-overexpressing group (Figure 2M), indicating that KIF14 enhances both the seeding and outgrowth of metastatic lesions. Collectively, these data establish KIF14 as a potent driver of CRC cell migration, invasion, and metastatic colonization *in vivo*.

At the molecular level, KIF14 depletion induced a shift toward an epithelial phenotype, as evidenced by increased E-cadherin and reduced N-cadherin and vimentin protein levels in siKIF14 cells (Supplementary Figure S2, left). Conversely, KIF14 overexpression

Table 1. Relationships between KIF14 expression and the clinicopathological features of CRC patients

		KIF14 expression		*P* value
		Low	High	
All patients	62	20(32.3%)	42(67.7%)	
Age				0.2524
	≤60	14(70%)	18(42.9%)	
	>60	6(30%)	24(57.1%)	
Gender				>0.9999
	Male	14(70%)	28(66.7%)	
	Female	6(30%)	14(33.3%)	
Histologic grade				0.3390
	Well differentiation	6(30%)	4(9.5%)	
	Moderate differentiation	12(60%)	34(81.0%)	
	Poor differentiation	2(10%)	4(9.5%)	
Stage				*0.0362*
	I	8(40%)	2(4.8%)	
	II	4(20%)	20(47.6%)	
	III/IV	8(40%)	20(47.6%)	
Lymphatic metastases				>0.9999
	Positive	10(50%)	24(57.1%)	
	Negative	10(50%)	18(42.9%)	
Perineural invasion				>0.9999
	Positive	2(10%)	8(19.0%)	
	Negative	18(90%)	34(81.0%)	

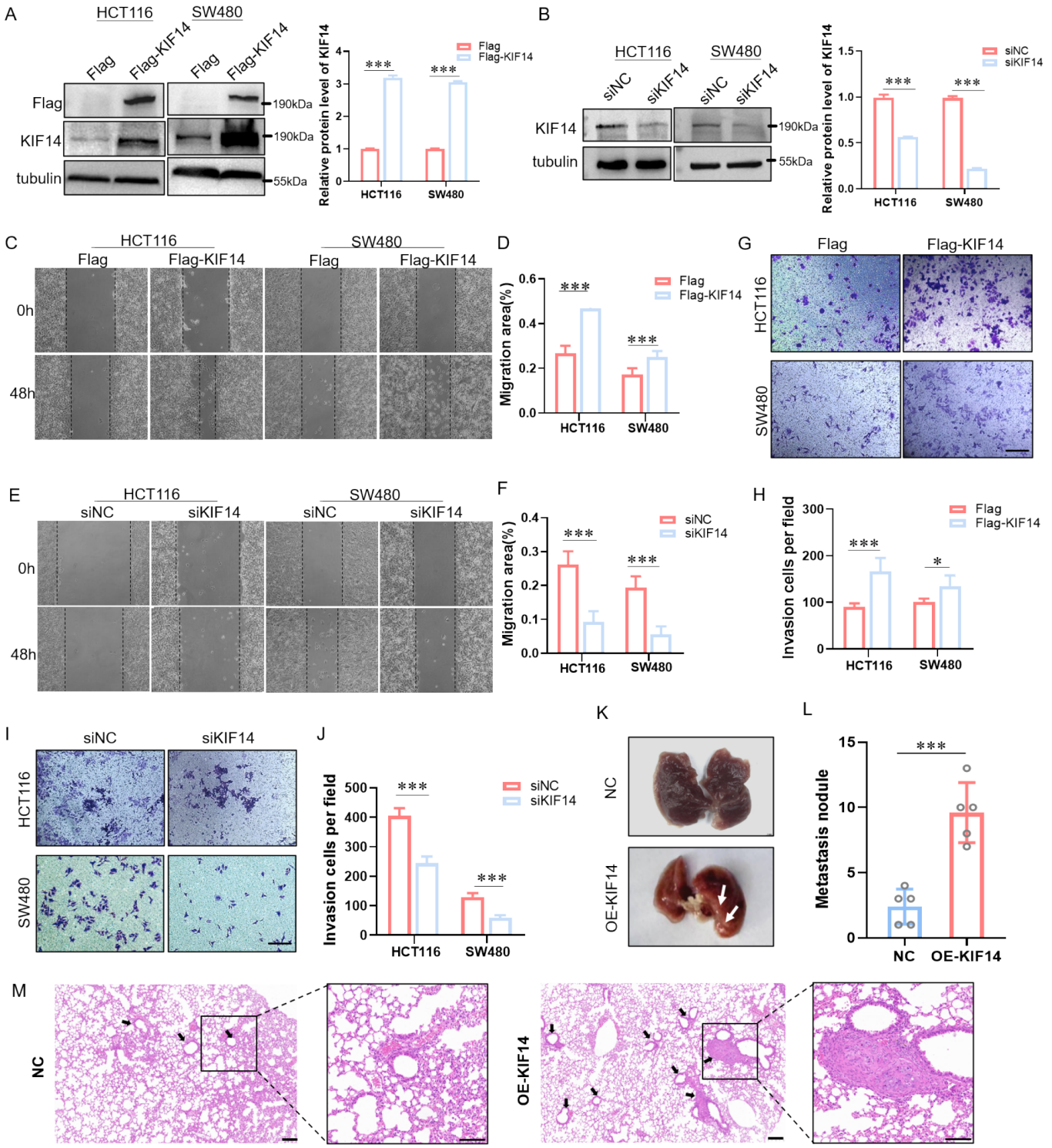

Figure 2. KIF14 promotes CRC cell migration and metastasis (A,B) Western blot analysis was performed to detect KIF14 protein expression levels in HCT116 and SW480 cells with KIF14 overexpression or *KIF14* knockdown. The band intensities for each condition were quantified via densitometry. (C,D) Wound healing assay in CRC cells after KIF14 overexpression. (E,F) Wound healing assay in CRC cells after *KIF14* knockdown. (G,H) Transwell invasion assay in CRC cells transfected with Flag or Flag-KIF14 (scale bar: 100 μm). (I,J) Transwell invasion assay under *KIF14* knockdown (scale bar: 100 μm). (K) Representative images showing the distribution of metastatic nodules ($n = 5$ per group). (L) Number of lung metastatic nodules per mouse. (M) Representative H&E staining of lung sections from mice injected with SW480-NC or SW480-OE-KIF14 cells. The arrows indicate metastatic nodules (scale bar: 200 μm). The data are presented as the mean ± SD. * $P < 0.05$, ** $P < 0.01$, *** $P < 0.001$.

promoted a mesenchymal phenotype, as indicated by elevated vimentin expression and decreased E-cadherin expression compared with those in the controls (Supplementary Figure S2, right). These findings identify KIF14 as a key regulator of EMT and CRC

metastasis both *in vitro* and *in vivo*.

KIF14 regulates colorectal cancer metastasis via adhesion signaling

To investigate the molecular basis of KIF14-mediated metastasis in colorectal cancer, we established SW480 cells with stable *KIF14* knockdown via lentiviral transduction. Efficient silencing was confirmed by western blot analysis (Figure 3A). RNA-seq analysis comparing KIF14-depleted cells (SW480-shKIF14) with control cells revealed 2545 DEGs (fold change ≥ 2, FDR ≤ 0.05; Figure 3B). Metastasis-suppressive transcripts such as COL6A2 and VAV1 were upregulated, whereas pro-metastatic drivers such as BIRC5, ITGA2, and vimentin were downregulated, indicating a shift toward decreased invasive potential.

Kyoto Encyclopedia of Genes and Genomes (KEGG) pathway enrichment highlighted the MAPK signaling pathway, cytokine–cytokine receptor interaction, and focal adhesion among the top hits (Figure 3C). The MAPK cascade—a well-known driver of tumor cell proliferation and survival—corroborates previous reports of KIF14-mediated growth in colorectal and other cancers [14,27,28]. The enrichment of cytokine–cytokine receptor interactions points to a potential role for KIF14 in reshaping the tumor microenvironment via inflammatory signaling. Gene Ontology (GO) analysis further revealed alterations in processes related to cell migration, extracellular matrix organization, and cytoskeletal structure (Figure 3D), which was consistent with cytoskeletal remodeling. Importantly, gene set enrichment analysis (GSEA) demonstrated robust enrichment of focal adhesion gene sets upon *KIF14* knockdown

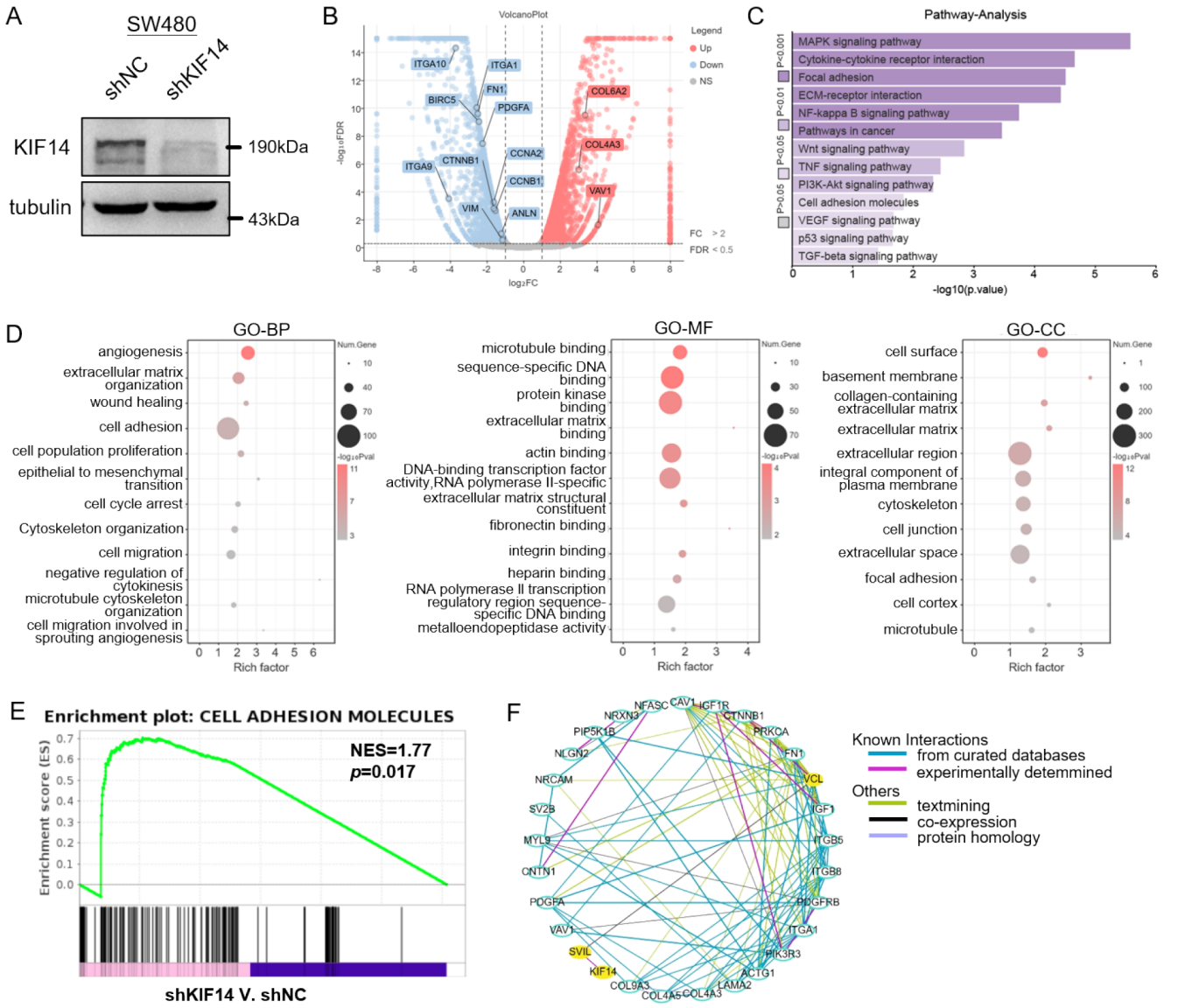

Figure 3. KIF14 promotes colorectal cancer metastasis through focal adhesion signaling (A) Western blot analysis confirming efficient *KIF14* knockdown in SW480 cells stably expressing shKIF14 or shNC. (B) Volcano plot of the DEGs between shKIF14-transfected cells and control cells. (C) KEGG pathway analysis of DEGs. (D) GO enrichment analysis of biological processes, molecular functions, and cellular components. (E) GSEA revealed significant enrichment of the cell adhesion molecule pathway (NES = 1.71, $P = 0.017$) in *KIF14*-knockdown cells. (F) PPI network of DEGs involved in focal adhesion signaling.

(NES = 1.77, $P = 0.017$; Figure 3E). Given its specific enrichment and direct link to cytoskeletal dynamics, we prioritized focal adhesion for downstream functional validation of the role of KIF14 in tumor cell motility.

Finally, protein–protein interaction (PPI) network analysis revealed a direct association between KIF14 and the cytoskeletal protein SVIL, which interfaces with the focal adhesion component vinculin (Figure 3F). Together, these transcriptomic insights support a model in which KIF14 modulates focal adhesion–related networks to drive CRC cell migration and invasion.

KIF14 modulates focal adhesion formation in colorectal cancer

Transcriptomic analysis via RNA-seq revealed that KIF14 depletion affected the expression of genes associated with focal adhesion. To experimentally validate this phenomenon, we examined the subcellular localization of KIF14 and vinculin, a canonical focal adhesion marker, via immunofluorescence microscopy. In control SW480 cells, endogenous KIF14 and vinculin strongly colocalized at the leading edge of migrating cells (Figure 4A). In contrast, SW480-shKIF14 cells displayed a diffuse cytoplasmic distribution of vinculin and markedly fewer, less mature focal adhesions. Quantitative analysis of the vinculin fluorescence intensity profiles confirmed the significant loss of vinculin enrichment at the cell front upon KIF14 depletion (Figure 4B). Moreover, morphometric measurements revealed that, compared with control cells, shKIF14 cells presented a >50% reduction in the average focal adhesion area ($P < 0.01$) and an approximately 66% decrease in the number of focal adhesions per cell ($P < 0.05$) (Figure 4C–D).

Conversely, restoring KIF14 expression via Flag-KIF14 in SW480 cells not only restored the peripheral localization of vinculin-marked focal adhesions but also promoted the formation of larger and more numerous adhesion complexes (Figure 4E–F). Compared with those of vector control cells, quantitative analysis revealed a significant increase in both the focal adhesion area and number of KIF14-overexpressing cells ($P < 0.01$; Figure 4G–H). These findings demonstrate that KIF14 regulates focal adhesion formation, providing a mechanistic explanation for its promigratory and noninvasive functions in CRC progression.

To further support a direct interaction between KIF14 and vinculin, coimmunoprecipitation experiments were performed. The results demonstrated that exogenously expressed Flag-KIF14 was able to pull down endogenous vinculin (Figure 4I), providing biochemical evidence for their association. Reciprocally, in 293T cells cotransfected with Flag-KIF14 and HA-vinculin, anti-HA immunoprecipitation efficiently pulled down Flag-KIF14 (Figure 4J), whereas HA- or Flag-vector controls had no Flag-KIF14, confirming a specific KIF14–vinculin interaction. Additionally, protein–protein interaction modeling via AlphaFold3 revealed potential hydrogen bond interactions between KIF14 and vinculin (Figure 4K), underscoring the structural basis of their interaction.

Identification of E2F1 as a transcriptional regulator of KIF14

Given the pivotal role of KIF14 in driving CRC progression and metastasis, we next sought to elucidate the upstream regulatory mechanisms responsible for its dysregulated expression in CRC. Bioinformatics analysis integrating the human TFBD and JASPAR databases revealed 31 candidate transcription factors significantly associated with elevated KIF14 expression (Figure 5A). Multiomics correlation analysis via the Colonomics database revealed that among these candidates, E2F1 is the factor most strongly correlated with KIF14 expression (Pearson r = 0.495, $P < 0.001$; Supplementary Table S3, Figure 5B).

Quantitative real-time PCR (qRT–PCR) analysis revealed that E2F1 overexpression significantly upregulated KIF14 mRNA levels in HCT116 and SW480 cells, with a more pronounced effect on SW480 cells ($P < 0.01$ and $P < 0.001$, respectively; Figure 5C). Conversely, siRNA-mediated *E2F1* knockdown markedly suppressed KIF14 transcription in both cell lines ($p < 0.001$; Figure 5D). At the protein level, transfection with siE2F1 for 72 h substantially decreased KIF14 expression in both HCT116 and SW480 cells ($P < 0.001$), whereas transfection with the pFlag-E2F1 plasmid significantly increased KIF14 protein levels in these cell lines (Figure 5E–F). These findings indicate that E2F1 is a key regulator of KIF14 expression in CRC cells.

E2F1 directly regulates KIF14 transcription through promoter binding

To investigate the molecular mechanism by which E2F1 regulates KIF14 expression, we initially searched for potential E2F1-binding sites on the *KIF14* promoter via the JASPAR database. This analysis revealed three putative E2F1 binding sites located at positions –497/–487, –1183/–1176, and –1315/–1305 base pairs (bp) relative to the transcription start site (TSS) (Figure 6A). To confirm the interaction between E2F1 and these sites, we conducted chromatin immunoprecipitation (ChIP) assays using cells stably expressing Flag-tagged E2F1. The results revealed specific enrichment of all three promoter regions by the E2F1 antibody, with enrichment levels significantly greater than those observed with the IgG controls. Furthermore, compared with wild-type cells, E2F1-overexpressing cells presented increased enrichment, providing strong evidence of the direct binding of E2F1 to the *KIF14* promoter (Figure 6B–C).

To assess the functional significance of the DNA-binding domain of E2F1, we created a pFlag-E132 mutant construct by performing site-directed mutagenesis on key residues (L132E/N133S) within this domain (Figure 6D–E). Subsequent ChIP assays revealed that these mutations disrupted the ability of E2F1 to bind to the *KIF14* promoter, and enrichment decreased to levels similar to those in the empty vector controls (Figure 6F).

To clarify the mechanism of KIF14 transcriptional regulation, we generated luciferase reporters containing the wild-type *KIF14* promoter and constructs with mutated E2F1-binding sites (Figure 6G). Luciferase assays revealed that E2F1 overexpression significantly increased *KIF14* promoter activity, whereas mutations at these sites progressively attenuated this effect (Figure 5H). Additionally, E2F1 overexpression increased *KIF14* promoter activity in a binding site-dependent manner, whereas a DNA-binding-defective E2F1 mutant abolished this effect, confirming direct transcriptional regulation via promoter interaction (Figure 6I).

The E2F1–KIF14 axis facilitates colorectal cancer cell migration and invasion by regulating focal adhesion formation

To investigate the functional relevance of the E2F1–KIF14 signaling cascade in CRC progression, we conducted epistatic rescue assays in the HCT116 and SW480 cell lines. Western blot analysis validated

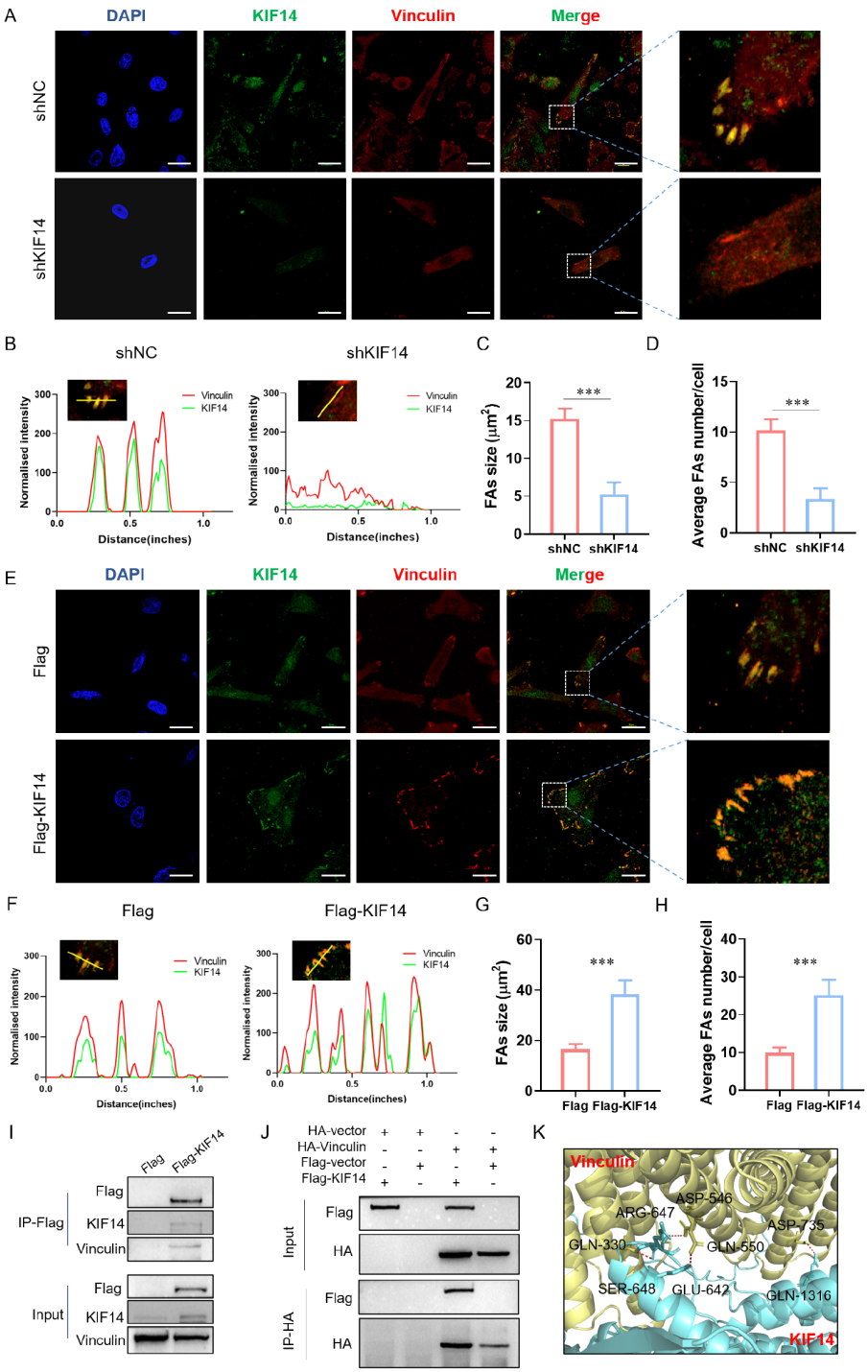

Figure 4. KIF14 positively regulates focal adhesion in colorectal cancer cells (A) Representative immunofluorescence images depicting the localization of KIF14 and vinculin in *KIF14*-knockdown or control SW480 cells. The nuclei were counterstained with DAPI. Insets show magnified views of the areas indicated by white boxes. (B) The intensity profiles of KIF14 and vinculin along the yellow line are presented in (A). (C,D) Quantification of the focal adhesion fluorescence area (C) and number (D) in the specified cell groups (n = 50 cells per condition from three independent experiments). (E) Representative immunofluorescence images depicting the localization of KIF14 and vinculin in SW480 cells subjected to KIF14 overexpression. (F) The intensity profiles of KIF14 and vinculin along the yellow line are presented in (E). (G,H) Quantification of the focal adhesion fluorescence area (C) and number (D) in the specified cell groups (n = 50 cells per condition from three independent experiments). (I) 293T cells expressing Flag-KIF14 or empty Flag were subjected to IP with Flag beads, followed by western blot analysis to detect vinculin. (J) Co-IP of Flag-KIF14 with HA-vinculin in 293T cells. The cells were co-transfected with Flag-KIF14 and HA-vinculin, and the lysates were immunoprecipitated with anti-HA beads, followed by western blot analysis with anti-Flag antibody. Co-transfection with HA-vector or Flag-vector served as a negative control. (K) Structural modeling reveals potential hydrogen bonds between KIF14 and Vinculin, suggesting that specific intermolecular interactions may contribute to their binding. Scale bar: 20 μm. The data are presented as the mean ± SD. * P < 0.05, ** P < 0.01, *** P <0.001.

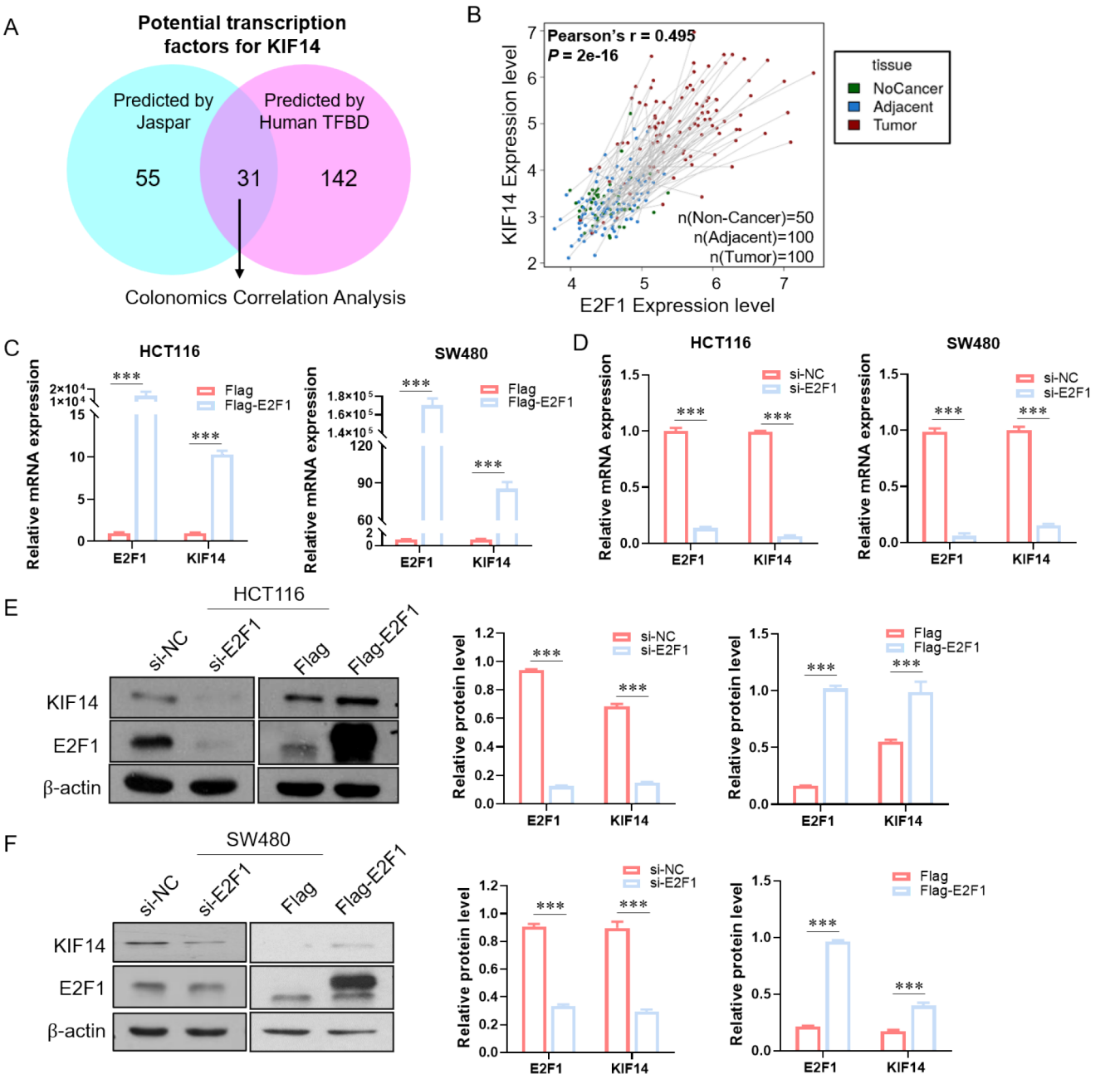

Figure 5. E2F1 regulates KIF14 expression in colorectal cancer cells (A) Venn diagram of potential regulators of KIF14 from the Human TFDB and JASPAR databases, with 31 common candidate TFs. (B) Colonomic database analysis revealed a strong positive correlation between E2F1 and KIF14 mRNA levels (Pearson r = 0.495, $P < 0.001$). (C–D) qRT–PCR analysis of *KIF14* mRNA following E2F1 overexpression (C) or siRNA knockdown (D) in HCT116 and SW480 cells. (E,F) Western blot analysis of E2F1 and KIF14 protein levels in HCT116 (E) and SW480 (F) cells after *E2F1* overexpression or knockdown. The data are shown as the mean ± SD; * $P < 0.05$, ** $P < 0.01$, *** $P < 0.001$.

the specificity and efficiency of our genetic interventions, confirming appropriate modulation of E2F1 and KIF14 protein expression across all experimental cohorts (Figure 7A–B).

Wound healing assays were also performed and demonstrated that *E2F1* knockdown substantially reduced the migratory capacity of both CRC cell lines compared with that of the controls (Figure 7C). Notably, this migration deficit was partially rescued by KIF14 overexpression in E2F1-depleted cells, establishing KIF14 as a critical downstream mediator of E2F1-dependent migration. Conversely, E2F1 overexpression increased motility, and this effect was significantly attenuated by *KIF14* knockdown (Figure 7D), underscoring the interdependence of these factors in CRC cell migration. Transwell invasion assays supported these findings: *E2F1* silencing impaired invasion, which was partially restored by KIF14 overexpression; similarly, E2F1-driven invasion was attenuated by *KIF14* knockdown (Figure 7E–F).

To clarify the underlying mechanism by which these factors exert their effects, we examined focal adhesion dynamics. Immunofluor-

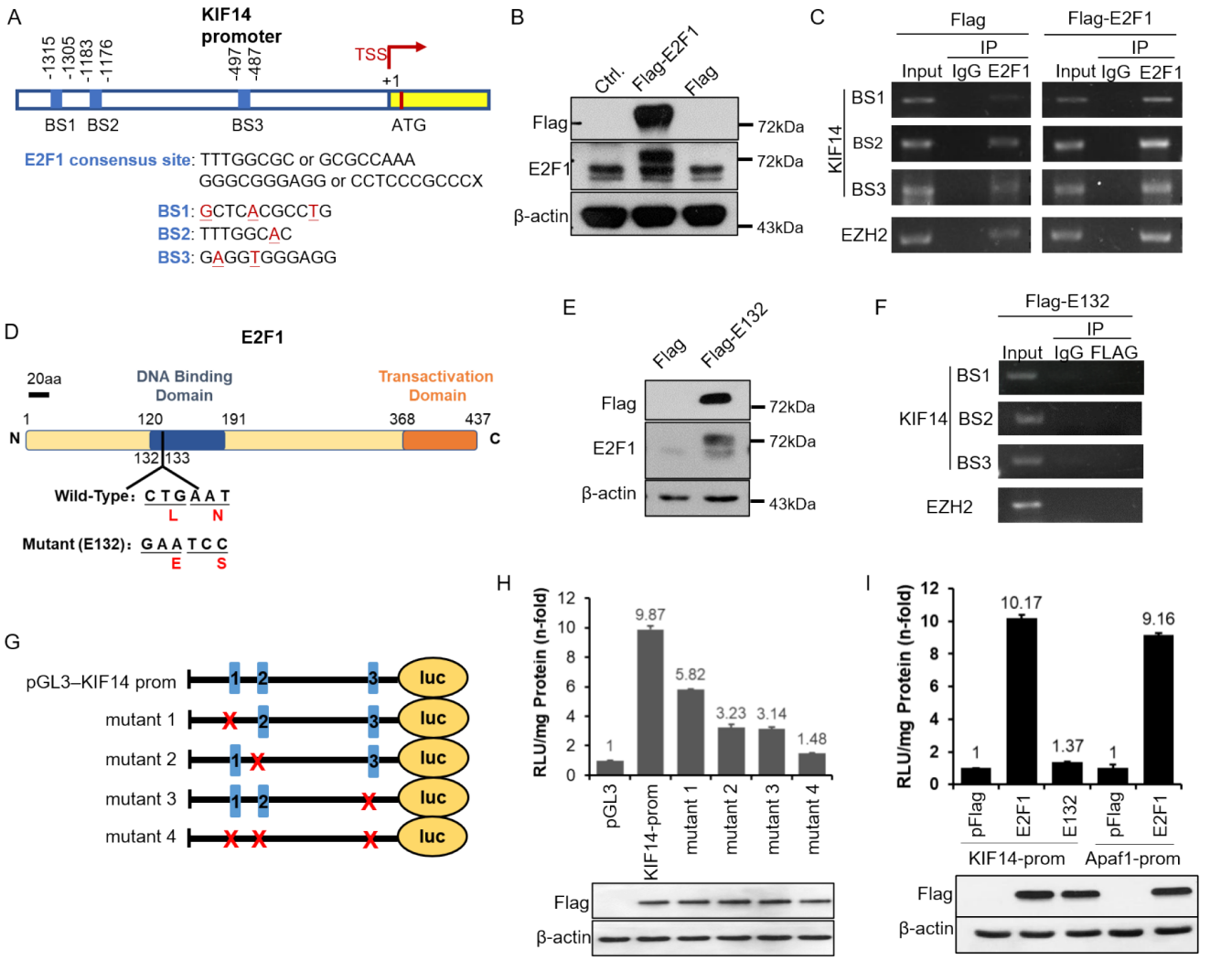

Figure 6. E2F1 activates KIF14 transcription by binding directly to its promoter (A) Three predicted E2F1 binding sites in the *KIF14* promoter (JASPAR analysis). (B) Western blot analysis confirming Flag-E2F1 expression, with β-actin used as a loading control. (C) ChIP assay showing E2F1 binding to the *KIF14* promoter in Flag-E2F1-expressing cells, with the *EZH2* promoter used as a positive control. (D) Schematic of the E2F1 DNA-binding domain mutant (E132: L132E/N133S). (E) Western blot analysis verifying the expression of wild-type and E132 mutant Flag-E2F1. (F) ChIP assay showing that the E132 mutant does not bind to the *KIF14* promoter. (G) Schematic of *KIF14* promoter luciferase constructs (WT and various mutants). (H) Luciferase activity in cells cotransfected with *E2F1* and *KIF14* promoter reporters; E2F1 protein expression was validated. (I) Comparison of the effects of wild-type and E132-mutant E2F1 on *KIF14* promoter activity (Apaf-1 was used as a positive control). The data are presented as the mean ± SD from three independent experiments. * $P < 0.05$, ** $P < 0.01$ (Student's *t* test).

escence analysis revealed that *E2F1* knockdown reduced the KIF14–vinculin colocalization rate at the leading edge of the cell (Figure 7G). Quantitative analysis confirmed decreased KIF14 enrichment and focal adhesion area, both of which were rescued by KIF14 expression restoration in E2F1-depleted cells (Figure 7H–I). Collectively, these findings establish the E2F1–KIF14 axis as a critical regulator of focal adhesion formation, cytoskeletal organization, migration, and invasion in CRC cells. Targeting this pathway may provide new opportunities for inhibiting CRC metastasis.

Discussion

Colorectal cancer (CRC) metastasis remains difficult to treat, and clarification of the underlying molecular mechanisms is critical for facilitating the development of targeted therapies. In this study, we revealed that the E2F1–KIF14 signaling axis plays a central role in orchestrating CRC metastasis through coordinated transcriptional activation and focal adhesion formation. In invasive CRC cells, E2F1 is upregulated and directly binds to the *KIF14* promoter, leading to upregulated KIF14 expression. KIF14, in turn, transports vinculin to the leading edge of the cell, promoting focal adhesion formation and enhancing cellular invasion. Conversely, in noninvasive CRC cells, lower E2F1 levels result in diminished KIF14 expression and vinculin mislocalization, thereby restricting invasive capacity (Figure 8).

Analysis of the clinical samples in our study revealed that KIF14 is significantly upregulated in CRC tissues and cell lines and that higher KIF14 expression strongly correlates with advanced tumor stage and poor overall survival, which is in line with previous reports [5,14,15]. At the cellular level, KIF14 expression was markedly increased in CRC cell lines compared with normal colonic

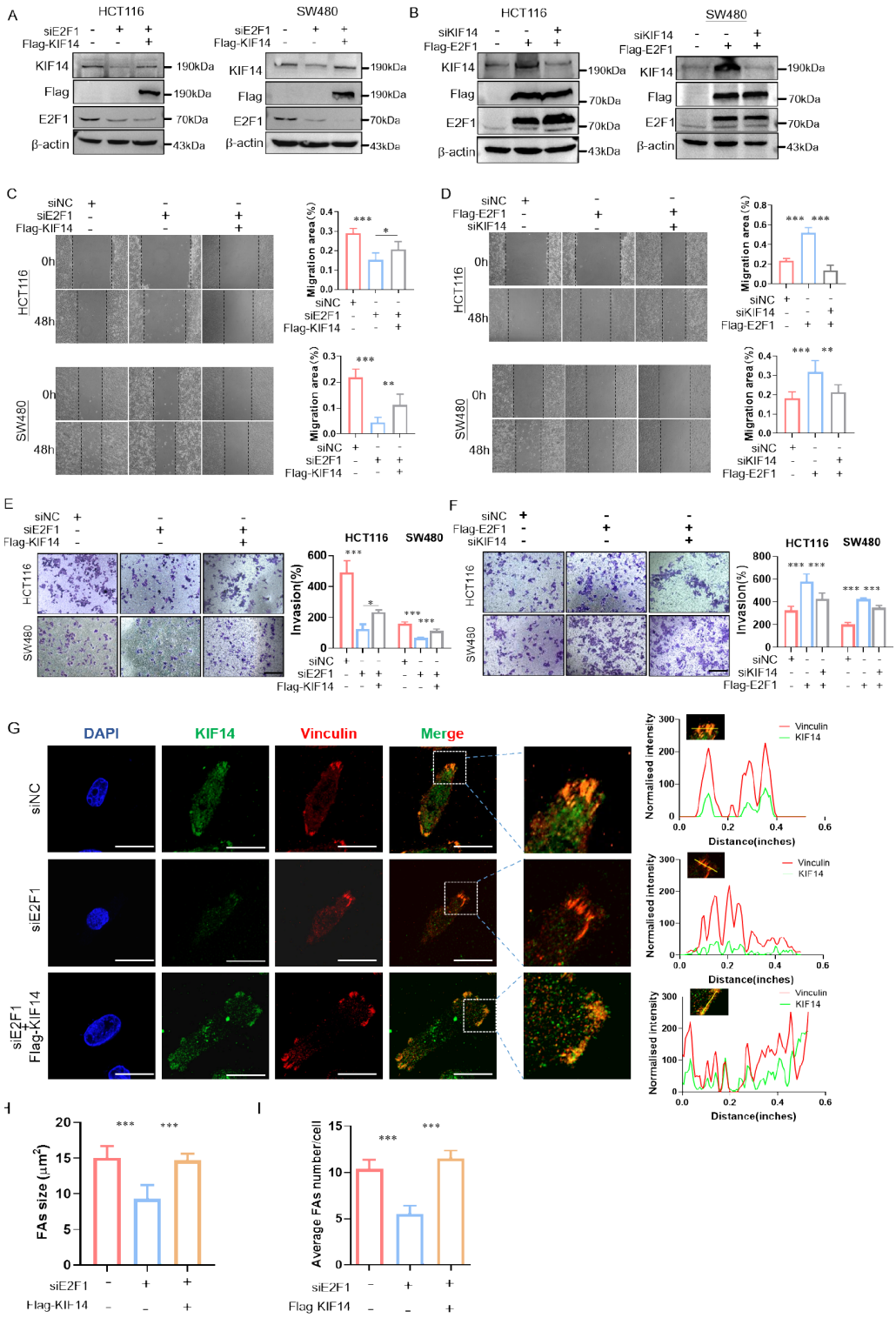

Figure 7. E2F1 regulates colorectal cancer cell migration and invasion via KIF14 (A) Western blot analysis confirming *E2F1* knockdown and rescue with KIF14 overexpression in HCT116 and SW480 cells. (B) Western blot analysis validating E2F1 overexpression and *KIF14* knockdown in CRC cells. (C,D) Scratch assay images at 0 and 48 h: (C) siE2F1 impaired migration, which was rescued by FlagKIF14; (D) FlagE2F1 promoted migration, which was reversed by siKIF14. (E-F) Transwell invasion: (E) siE2F1 reduces invasion, which is partially restored by FlagKIF14; (F) FlagE2F1 enhances invasion, which is attenuated by siKIF14. Scale bar: 100 μm. (G) Representative immunofluorescence images showing KIF14 and vinculin localization in SW480 cells transfected with control siRNA, E2F1 siRNA, or a combination of E2F1 siRNA and the KIF14 expression vector. Scale bar: 20 μm. The intensity profiles of KIF14 and vinculin along the yellow line. (H,I) Quantification of the focal adhesion fluorescence area (H) and number (I) in the indicated experimental groups (n=50 cells per condition from three independent experiments). * $P < 0.05$, ** $P < 0.01$, *** $P < 0.001$.

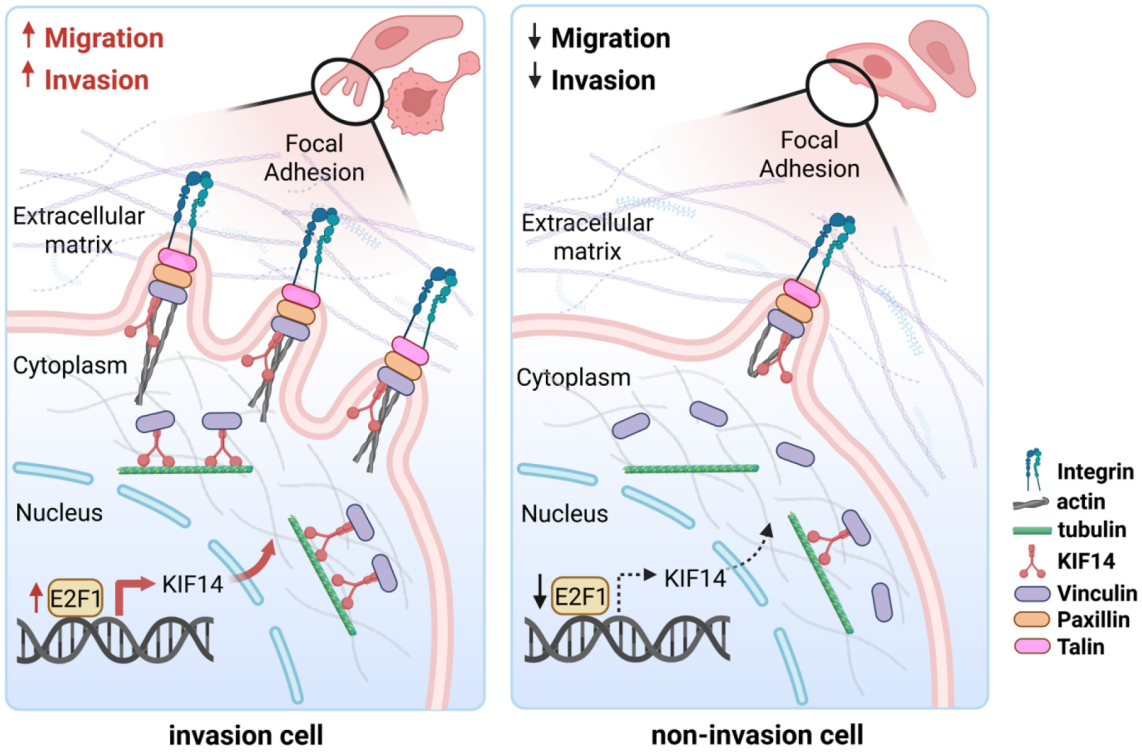

Figure 8. E2F1-mediated upregulation of KIF14 promotes CRC invasion by enhancing focal adhesion formation

epithelial cells. Notably, among CRC cell lines, HCT116 and SW480—typically less metastatic—exhibit higher basal KIF14 expression than do the more metastatic SW620 and LoVo cells, suggesting a context-dependent role for KIF14 in metastatic progression. Functionally, KIF14 overexpression significantly accelerated wound healing and invasion *in vitro*, whereas *KIF14* knockdown impaired these processes. *In vivo*, KIF14-overexpressing SW480 cells formed more and larger metastatic nodules in the lung, substantiating the prometastatic role of KIF14.

Transcriptome analysis revealed that KIF14 promotes tumor cell metastasis by regulating focal adhesion formation and activating cell adhesion-related pathways. This finding is consistent with previous studies in gastric and breast cancer models, where KIF14 was shown to modulate integrin-mediated cell adhesion and cytoskeletal dynamics. For example, in breast cancer, KIF14 directly interacts with the Rap1 effector Radil to regulate Rap1-dependent integrin activation, thereby influencing cell adhesion and migratory behavior [11]. These results suggest that KIF14 plays a broad and crucial role in the regulation of adhesion-related signaling beyond its well-known function in mitosis.

In this study, we further demonstrated that KIF14 facilitates the assembly of focal adhesions at the leading edge of migrating cells. Immunofluorescence analysis revealed that *KIF14* knockdown caused the diffuse distribution of vinculin in the cytoplasm and suppressed focal adhesion formation, whereas KIF14 overexpression restored and enhanced vinculin accumulation at the cell periphery. Importantly, our coimmunoprecipitation assays confirmed a direct physical interaction between KIF14 and vinculin, suggesting a molecular basis for these observations. In addition to its classic role as a microtubule motor, KIF14 uses its N-terminal extension to bind to F-actin, indicating a dual role in cytoskeletal dynamics [7]. KIF14 may function as a molecular bridge, connecting F-actin to vinculin to support focal adhesion assembly and maturation. By reinforcing cell–ECM attachments and enhancing mechanotransduction, this mechanism increases cancer cell invasiveness.

Growing evidence underscores the important roles of cell adhesion molecules and focal adhesions in tumor progression and metastasis, as they mediate not only cell–cell and cell–ECM interactions but also processes such as intravasation, EMT, and metastatic colonization [29–32]. Although vinculin is a classic component of focal adhesions, its subcellular localization rather than its overall expression appears to be more influential in tumor cell migration and invasion. For example, shifting vinculin from cell junctions to focal adhesions enhances migratory potential in breast cancer models [33]. Our results indicate that KIF14 modulates the distribution of vinculin-positive adhesion complexes, suggesting a role in focal adhesion dynamics during cancer cell motility, although the precise molecular mechanisms by which KIF14 orchestrates cytoskeletal reorganization and vinculin recruitment during metastasis warrant further investigation.

Bioinformatics profiling revealed that E2F1 is the top transcriptional regulator of KIF14, a finding we confirmed via ChIP and luciferase assays: wild-type E2F1 binds to three discrete sites in the *KIF14* promoter and drives its transcription, whereas mutation of E2F1's DNA-binding domain abolishes both binding and reporter activation. E2F1 is well known to orchestrate oncogenic programs, including cell cycle progression, EMT and invasion, via targets such as ZEB1 and SNAI1 in diverse cancers, and high E2F1 levels in CRC correlate with advanced stage and poor prognosis [34–37]. Our work extends this paradigm, showing that E2F1 not only promotes EMT but also directly upregulates KIF14 to control focal adhesion

assembly. Silencing of *E2F1* suppressed KIF14 expression, decreased focal adhesion integrity and vinculin localization, and impaired cell migration and invasion; conversely, restoring KIF14 expression in E2F1-depleted cells rescued focal adhesion formation and partially restored invasive behavior.

In summary, our work identified the E2F1–KIF14 axis as a master regulator of focal adhesion formation and CRC metastasis. Through transcriptional upregulation of KIF14 by E2F1, KIF14 promotes focal adhesion assembly and promotes the migration and invasion of CRC cells. These findings expand our understanding of the molecular mechanisms underlying CRC metastasis and highlight the E2F1–KIF14 signaling axis as a promising therapeutic target whose inhibition may simultaneously impair focal adhesion dynamics, cell motility, and invasive potential.

Supplementary Data

Supplementary data is available at *Acta Biochimica et Biophysica Sinica* online.

Funding

This work was supported by the grant from the National Natural Science Foundation of China (No. 81703013).

Conflict of Interest

The authors declare that they have no conflict of interest.

References

1. Bray F, Laversanne M, Sung H, Ferlay J, Siegel RL, Soerjomataram I, Jemal A. Global cancer statistics 2022: GLOBOCAN estimates of incidence and mortality worldwide for 36 cancers in 185 countries. *CA Cancer J Clin* 2024, 74: 229–263
2. Akimoto N, Ugai T, Zhong R, Hamada T, Fujiyoshi K, Giannakis M, Wu K, *et al.* Rising incidence of early-onset colorectal cancer — a call to action. *Nat Rev Clin Oncol* 2021, 18: 230–243
3. Siegel RL, Wagle NS, Cercek A, Smith RA, Jemal A. Colorectal cancer statistics, 2023. *CA Cancer J Clin* 2023, 73: 233–254
4. Benoit MPMH, Asenjo AB, Paydar M, Dhakal S, Kwok BH, Sosa H. Structural basis of mechano-chemical coupling by the mitotic kinesin KIF14. *Nat Commun* 2021, 12: 3637
5. B.L. Thériault, T.W. Corson, Kif14: A Clinically Relevant Kinesin and Potential Target for Cancer Therapy, in: F.S.B.F. Kozielski (Ed.), Kinesins and Cancer, Springer Netherlands, *Dordrecht* 2015, 149–170
6. Gruneberg U, Neef R, Li X, Chan EHY, Chalamalasetty RB, Nigg EA, Barr FA. KIF14 and citron kinase act together to promote efficient cytokinesis. *J Cell Biol* 2006, 172: 363–372
7. Samwer M, Dehne HJ, Spira F, Kollmar M, Gerlich DW, Urlaub H, Görlich D. The nuclear F-actin interactome of Xenopus oocytes reveals an actin-bundling kinesin that is essential for meiotic cytokinesis. *EMBO J* 2013, 32: 1886–1902
8. Corson TW, Huang A, Tsao MS, Gallie BL. KIF14 is a candidate oncogene in the 1q minimal region of genomic gain in multiple cancers. *Oncogene* 2005, 24: 4741–4753
9. Jiang W, Wang J, Yang X, Shan J, Zhang Y, Shi X, Wang Y, *et al.* KIF14 promotes proliferation, lymphatic metastasis and chemoresistance through G3BP1/YBX1 mediated NF-κB pathway in cholangiocarcinoma. *Oncogene* 2023, 42: 1392–1404
10. Xiao L, Zhang S, Zheng Q, Zhang S. Dysregulation of KIF14 regulates the cell cycle and predicts poor prognosis in cervical cancer: A study based on integrated approaches. *Braz J Med Biol Res* 2021, 54: e11363
11. Ahmed SM, Thériault BL, Uppalapati M, Chiu CWN, Gallie BL, Sidhu SS, Angers S. KIF14 negatively regulates Rap1a–Radil signaling during breast cancer progression. *J Cell Biol* 2012, 199: 951–967
12. Yang Z, Li C, Yan C, Li J, Yan M, Liu B, Zhu Z, *et al.* KIF14 promotes tumor progression and metastasis and is an independent predictor of poor prognosis in human gastric cancer. *Biochim Biophys Acta Mol Basis Dis* 2019, 1865: 181–192
13. Zhao Q, Chen S, Chen L. LETM1 (leucine zipper-EF-hand-containing transmembrane protein 1) silence reduces the proliferation, invasion, migration and angiogenesis in esophageal squamous cell carcinoma via KIF14 (kinesin family member 14). *Bioengineered* 2021, 12: 7656–7665
14. Wang ZZ, Yang J, Jiang BH, Di JB, Gao P, Peng L, Su XQ. KIF14 promotes cell proliferation via activation of Akt and is directly targeted by miR-200c in colorectal cancer. *Int J Oncol* 2018, 1939: 1952
15. Qin K, Luo JY, Zeng DT, Huang WY, Li B, Li Q, Zhan YT, *et al.* Kinesin family member 14 expression and its clinical implications in colorectal cancer. *World J Gastrointest Oncol* 2025, 17: 102696
16. Kosinski J, Sechi A, Hain J, Villwock S, Ha SA, Hauschulz M, Rose M, *et al.* ITIH5 as a multifaceted player in pancreatic cancer suppression, impairing tyrosine kinase signaling, cell adhesion and migration. *Mol Oncol* 2024, 18: 1486–1509
17. Kanchanawong P, Shtengel G, Pasapera AM, Ramko EB, Davidson MW, Hess HF, Waterman CM. Nanoscale architecture of integrin-based cell adhesions. *Nature* 2010, 468: 580–584
18. Hoffmann M, Schwarz US. A kinetic model for RNA-interference of focal adhesions. *BMC Syst Biol* 2013, 7: 2
19. Liu Z, Zhang X, Ben T, Li M, Jin Y, Wang T, Song Y. Focal adhesion in the tumour metastasis: From molecular mechanisms to therapeutic targets. *Biomark Res* 2025, 13: 38
20. Crowley JL, Smith TC, Fang Z, Takizawa N, Luna EJ, Brugge J. Supervillin reorganizes the actin cytoskeleton and increases invadopodial efficiency. *Mol Biol Cell* 2009, 20: 948–962
21. Díez-Villanueva A, Sanz-Pamplona R, Solé X, Cordero D, Crous-Bou M, Guinó E, Lopez-Doriga A, *et al.* COLONOMICS - integrative omics data of one hundred paired normal-tumoral samples from colon cancer patients. *Sci Data* 2022, 9: 595
22. Győrffy B, Surowiak P, Budczies J, Lánczky A, Chellappan SP. Online survival analysis software to assess the prognostic value of biomarkers using transcriptomic data in non-small-cell lung cancer. *PLoS ONE* 2013, 8: e82241
23. Wang Y, Zhou B, Lian X, Yu S, Huang B, Wu X, Wen L, *et al.* KIF18A is a novel target of JNK1/c-jun signaling pathway involved in cervical tumorigenesis. *J Cell Physiol* 2025, 240: e31516
24. Rauluseviciute I, Riudavets-Puig R, Blanc-Mathieu R, Castro-Mondragon JA, Ferenc K, Kumar V, Lemma RB, *et al.* JASPAR 2024: 20th anniversary of the open-access database of transcription factor binding profiles. *Nucleic Acids Res* 2024, 52: D174–D182
25. Shen WK, Chen SY, Gan ZQ, Zhang YZ, Yue T, Chen MM, Xue Y, *et al.* AnimalTFDB 4.0: A comprehensive animal transcription factor database updated with variation and expression annotations. *Nucleic Acids Res* 2023, 51: D39–D45
26. Helin K, Wu CL, Fattaey AR, Lees JA, Dynlacht BD, Ngwu C, Harlow E. Heterodimerization of the transcription factors E2F-1 and DP-1 leads to cooperative trans-activation.. *Genes Dev* 1993, 7: 1850–1861
27. Ge J, Dai J, Ji H, Guo J, Shen X, Sun D, Chen Q, *et al.* Identification of tRF-29-79MP9P9NH525 as a biomarker and tumor suppressor of gastric cancer via regulating KIF14/AKT pathway. *Cell Death Discov* 2025, 11: 238
28. Singel SM, Cornelius C, Zaganjor E, Batten K, Sarode VR, Buckley DL, Peng Y, *et al.* KIF14 promotes AKT phosphorylation and contributes to

chemoresistance in triple-negative breast cancer. *Neoplasia* 2014, 16: 247–256.e2
29. Eke I, Cordes N. Focal adhesion signaling and therapy resistance in cancer. *Semin Cancer Biol* 2015, 31: 65–75
30. Janiszewska M, Primi MC, Izard T. Cell adhesion in cancer: Beyond the migration of single cells. *J Biol Chem* 2020, 295: 2495–2505
31. Sun Z, Lambacher A, Fässler R. Nascent adhesions: from fluctuations to a hierarchical organization. *Curr Biol* 2014, 24: R801–R803
32. Parsons JT, Horwitz AR, Schwartz MA. Cell adhesion: Integrating cytoskeletal dynamics and cellular tension. *Nat Rev Mol Cell Biol* 2010, 11: 633–643
33. Villeneuve C, Lagoutte E, de Plater L, Mathieu S, Manneville JB, Maître JL, Chavrier P, ***et al.*** aPKCi triggers basal extrusion of luminal mammary epithelial cells by tuning contractility and vinculin localization at cell junctions. *Proc Natl Acad Sci USA* 2019, 116: 24108–24114
34. Huang P, Wen F, Li Q. Current concepts of the crosstalk between lncRNA and E2F1: shedding light on the cancer therapy. *Front Pharmacol* 2024, 15: 1432490
35. Gong H, Lu F, Zeng X, Bai Q. E2F transcription factor 1 (E2F1) enhances the proliferation, invasion and EMT of trophoblast cells by binding to Zinc Finger E-Box Binding Homeobox 1 (ZEB1). *Bioengineered* 2022, 13: 2360–2370
36. Wang Z, Tang P, Xiao H, Peng S, Chen J, Wang Y, Xu J, ***et al.*** Histone demethylasePHF8 promotes prostate cancer metastasis via theE2F1 – SNAI1 axis. *J Pathol* 2024, 264: 68–79
37. Zhou C, Liu H, Wang F, Hu T, Liang Z, Lan N, He X, ***et al.*** circCAMSAP1 Promotes Tumor Growth in Colorectal Cancer via the miR-328-5p/E2F1 Axis. *Mol Ther* 2020, 28: 914–928